Conformation-Induced Electrical Bistability in Non-conjugated Polymers with Pendant Carbazole Moieties

Siew Lay Lim,[†,‡] Qidan Ling,[‡] Eric Yeow Hwee Teo,[§] Chun Xiang Zhu,[§] Daniel Siu Hung Chan,[§] En-Tang Kang,*[,‡] and Koon Gee Neoh[‡]

NUS Graduate School of Integrative Sciences and Engineering (NGS), Department of Chemical and Biomolecular Engineering, and SNDL, Department of Electrical and Computer Engineering, National University of Singapore, 10 Kent Ridge, Singapore 119260

Received June 7, 2007. Revised Manuscript Received July 18, 2007

Conformation-induced volatile and nonvolatile conductance switching effects were demonstrated in non-conjugated polymers containing the same electroactive pendant groups. Single-layer devices of the structure indium-tin-oxide/polymer/aluminum were fabricated from two non-conjugated polymers with pendant carbazole groups in different spacer units. The device based on poly(2-(*N*-carbazolyl)ethyl methacrylate) (PMCz) exhibited nonvolatile write-once-read-many-times (WORM) memory behavior with an ON/OFF current ratio up to 10^6, while the device based on poly(9-(2-((4-vinylbenzyl)oxy)ethyl)-9*H*-carbazole) (PVBCz) exhibited volatile memory behavior with an ON/OFF current ratio of approximately 10^3. The formation of carbazole excimers resulting from conformation-induced conductance switching under an electric field was revealed in situ by fluorescence spectroscopy. The corresponding voltage-induced conformation ordering in the polymer film was captured by transmission electron microscopy. In the absence of a spacer unit between the pendant carbazole group and the main chain, regioregular poly(*N*-vinylcarbazole) (PVK) exhibited only one conductivity state (ON state). The differences in memory behavior among the three polymers were attributed to their inherent differences in the degree of regioregularity and ease of conformational relaxation of the field-induced regioregular carbazole groups. These conformational effects were in turn dictated by the chemical structure and steric effect of the spacer unit between the pendant carbazole group and the main chain.

Introduction

Organic and polymeric materials have been used as alternatives to traditional Si, Ge, and GaAs semiconductors in the fabrication of electronic devices, such as light-emitting diodes,[1−3] transistors,[4] lasers,[5] sensors,[6] photovoltaic cells,[7,8] switches,[9] and memory devices.[10−13] Organic materials exhibiting electrically bistable behavior[14] are also alternatives for future data storage applications. Instead of information storage and retrieval by encoding "0" and "1" as the amount of charges stored in a cell in silicon devices, polymer memory devices store data in another form, for example, based on the high and low conductivity response to an external voltage. In comparison to inorganic materials, organic materials offer the potential advantages of low cost, good processability, and property-tuning by molecular design and appropriate syntheses.[15,16] Also, polymeric memory devices exhibit good scalability, can be stacked 3-dimensionally for high-density data storage, and can be fabricated into flexible devices.[14,17] In the field of organic and polymeric memory devices, molecular design and doping have been used in the fabrication of memory devices to achieve different memory properties.[18] The basic device mechanisms proposed for the observed conductance switching include charge-transfer,

* To whom correspondence should be addressed. Tel: +65-6874-2189. Fax: +65-6779-1936. E-mail: cheket@nus.edu.sg.
† NUS Graduate School of Integrative Sciences and Engineering (NGS).
‡ Department of Chemical and Biomolecular Engineering.
§ SNDL, Department of Electrical and Computer Engineering.

(1) Aguirre, C. M.; Auvray, S.; Pigeon, S.; Izquierdo, R.; Desjardins, P.; Martel, R. *Appl. Phys. Lett.* **2006**, *88*, Art. No. 183104.
(2) William, E. L.; Haavisto, K.; Li, J.; Jabbour, G. E. *Adv. Mater.* **2007**, *19*, 197.
(3) Lowry, M. S.; Goldsmith, J. I.; Slinker, J. D.; Rohl, R.; Pascal, R. A., Jr.; Malliaras, G. G.; Bernhard, S. *Chem. Mater.* **2005**, *17*, 5712.
(4) Drolet, N.; Morin, J. F.; Leclerc, N.; Wakim, S.; Tao, Y.; Leclerc, M. *Adv. Funct. Mater.* **2005**, *15*, 1671.
(5) Polson, R. C.; Vardeny, Z. V. *Appl. Phys. Lett.* **2004**, *85*, 1892.
(6) Juan, Z.; Swager, T. M. *Adv. Polym. Sci.* **2005**, *177*, 151.
(7) Hasobe, T.; Fukuzumi, S.; Kamat, P. V. *Angew. Chem., Int. Ed.* **2006**, *45*, 755.
(8) Roberson, L. B.; Poggi, M. A.; Kowalik, J.; Smestad, G. P.; Bottomley, L. A.; Tolbert, Coord, L. M. *Chem. Rev.* **2004**, *248*, 1491.
(9) Coe, S.; Woo, W. K.; Bawendi, M.; Bulovic, V. *Nature (London)* **2002**, *420*, 800.
(10) Yang, Y.; Ouyang, J.; Ma, L. P.; Tseng, R. J. H.; Chu, C. W. *Adv. Funct. Mater.* **2006**, *16*, 1001.
(11) Kanwal, A.; Chhowalla, M. *Appl. Phys. Lett.* **2006**, *89*, Art. No. 203103.
(12) Wang, H. P.; Pigeon, S.; Izquierdo, R.; Martel, R. *Appl. Phys. Lett.* **2006**, *89*, 183502.
(13) Bozano, L. D.; Kean, B. W.; Beinhoff, M.; Carter, K. R.; Rice, P. M.; Scott, J. C. *Adv. Funct. Mater.* **2005**, *15*, 1933.
(14) Stikeman, A. *Technol. Rev.* **2002**, *105*, 31.
(15) Raymo, F. M. *Adv. Mater.* **2002**, *14*, 401.
(16) Forrest, S. R. *Nature* **2004**, *428*, 911.
(17) Moller, S.; Perlov, C.; Jackson, W.; Taussig, C.; Forrest, S. R. *Nature*, **2003**, *426*, 166.
(18) (a) Bandyopadhyay, A.; Pal, A. J. *Chem. Phys. Lett.* **2003**, *371*, 86. (b) Bandhopadhyay, A.; Pal, A. J. *J. Phys. Chem. B* **2003**, *107*, 2531. (c) Ouyang, J.; Chu, C. −W.; Szmanda, C. R.; Ma, L.; Yang Y. *Nat. Mater.* **2004**, *3*, 918. (d) Majee, S. K.; Bandyopadhyay, A.; Pal, A. J. *Chem. Phys. Lett.* **2004**, *399*, 284. (e) Majumdar, H. S.; Baral, J. K.; Osterbacka, R.; Stubb, H. *Org. Electron.* **2005**, *6*, 188.(f) Lai, Q. X.; Zhu, Z. H.; Chen, Y.; Patil, S.; Wudl, F. *Appl. Phys. Lett.* **2006**, *88*, Art. 133515. (g) Patil, S.; Lai, Q. X.; Marchioni, F.; Jung, M. Y.;, Zhu, Z. H.; Chen, Y.; Wudl, F. *J. Mater. Chem.* ***2006****, 16, 4160.*

10.1021/cm071520x CCC: $37.00
Published on Web 09/21/2007

electroreduction, and charge tunneling. Although conductance switching based on single molecules and thin films of organic compounds, such as azobenzenes, rotaxane, Rose Bengal, and phenylene ethynylene oligomers, has been widely reported,[19−22] conformation-induced conductance switching for polymer memory device application has yet to be explored in detail.

Carbazole-containing polymers have been used in various technological applications because of the unique electronic and photochemical properties of the carbazole molecules.[23−24] The photoconductive properties of carbazole-containing polymers and their ability to transport positive charges (holes) are exploited in many applications, such as in the electrophotographic process and in light-emitting, photorefractive, and photovoltaic devices.[23] The carbazole molecule is also a well-known electron-donor and hole-transporting group.[25] In addition to applications in holographic data storage and information processing,[26] carbazole-containing polymers and complexes have been used in single-layer memory devices, such as nonvolatile polymer flash memory devices[27,28] and a write-once-read-many-times (WORM) memory device.[29]

In this work, we illustrate the effect of chemical structure on the conformation-induced switching properties of two non-conjugated polymers with pendant carbazole groups in different spacer units. Poly(*N*-vinylcarbazole) (PVK) is used as a reference. In the bulk polymer, carriers (holes) have a higher interchain mobility when the overlapping of related orbitals is large between two adjacent carbazole rings, and the disordered regions, in which carbazole rings do not stack regularly, act as trapping sites for carriers.[30] With the increases in spacer length and steric effect between the carbazole group and the polymer backbone, the electrical behavior observed upon application of an external bias to the device changes from that of a single conductivity state (for PVK) to that of the nonvolatile bistable states (for poly(2-(*N*-carbazolyl)ethyl methacrylate, or PMCz) and then to that of the volatile bistable states (for poly(9-(2-((4-vinylbenzyl)oxy)ethyl)-9*H*-carbazole, or PVBCz). We have previously observed bistable electrical switching in the PMCz device.[29] With the volatile switching behavior observed in the present work for the PVBCz device, the mechanism of conductance switching, based on the electric field-induced change in conformational regioregularity of the pendant carbazole groups, is ascertained by in situ fluorescence spectroscopy and high-resolution transmission electron microscopy measurements of the polymer films in the field-induced bistable states.

Experimental Section

Methods and Materials. Fourier transform infrared (FT-IR) spectroscopy was performed on a Shimadzu FTIR-8400 spectrophotometer. A mixture containing 100 mg of potassium bromide (KBr) and 1−2 mg of a polymer was ground into fine powder and compressed to form a transparent pellet for the FT-IR measurement. The weight-average molecular weight (M_w) and the corresponding polydispersity index (PDI) of each polymer were obtained by gel permeation chromatography (GPC) on a Waters GPC system, equipped with a Waters 1515 HPLC pump, a Waters 2414 refractive index detector, and Styragel HR 4E, HR 5E, and HR 6 GPC columns packed with rigid 5 μm styrene divinylbenzene particles. Tetrahydrofuran was used as the mobile phase, and polystyrene standards were used to calibrate the system. X-ray diffraction (XRD) analysis was performed on powder samples using a Shimadzu XRD-6000 spectrometer with a Cu Kα monochromatic radiation source at 40 kV and 30 mA. The 2θ angle was scanned from 0 to 80°. Glass transition temperatures (T_g) of the polymers were determined by differential scanning calorimetry on a Mettler Toledo DSC822e scanning calorimeter.

The UV−vis absorption spectra of the polymers in dilute THF solutions were obtained on a Shimadzu UV-3101 PC spectrophotometer. Cyclic voltammetry was performed using an Autolab potentiostat/galvanostat under an argon atmosphere. A thin polymer film was coated on the Pt disk electrode and was scanned anodically and cathodically in a 0.1 M acetonitrile solution of tetrabutylammonium hexafluorophosphate, with Ag/Ag^+ and a platinum wire as the reference and counterelectrodes, respectively. Simulated 3D models from molecular mechanics were obtained using the Bio-rad Sadtler Suite, version 1.0, and SymApps 6.0 softwares.

All polymers used were synthesized by free-radical homopolymerization of the respective monomers in dry tetrahydrofuran (THF) for 72 h at 65 °C, with 1 mol/L monomer feed concentration and azobisisobutyronitrile as the initiator, under an argon atmosphere. Each polymer was precipitated in methanol and purified by Soxhlet extraction with methanol. Poly(*N*-vinylcarbazole) (PVK) was synthesized by polymerization of 9-vinylcarbazole (98%). [FT-IR spectroscopy results (KBr pellet, cm^{-1}, ν-stretching): 3045, 3021, 2694, 2930 (ν(C−H) aliphatic); 1482, 1451 (ν(C═C) aromatic); 745, 718 (ν(C−H) carbazole). GPC: $M_w \approx 12\,000$ g mol^{-1}, PDI ≈ 1.5]. 2-(*N*-carbazolyl)ethyl methacrylate and the corresponding polymer, PMCz, were synthesized as reported.[29] [For PMCz, FT-IR spectroscopy results (KBr pellet, cm^{-1}): 3050, 2938 (ν(C−H) aliphatic); 1729 (ν(C═O)); 750, 724 (ν(C−H) carbazole). GPC: $M_w \approx 15\,800$ g mol^{-1}, PDI ≈ 2.7]. For the preparation of the 9-(2-((4-vinylbenzyl)oxy)ethyl)-9*H*-carbazole monomer,[31] 9*H*-carbazole-9-ethanol (97%, 5.6 g or 25.2 mmol) and sodium hydride (95%, 1.0 g or 41.7 mmol) were dissolved in THF. 4-Vinylbenzyl chloride (97%, 4.0 mL or 25.6 mmol) was added in one portion, and the solution was stirred in a 60 °C oil bath for 24 h under an argon atmosphere. The excess solvent was evaporated, and the

(19) Choi, B.−Y.; Kahng, S.−J.; Kim, S.; Kim, H.; Kim, H. W.; Song, Y. J.; Ihm, J.; Kuk, Y. *Phys. Rev. Lett.* **2006**, *96*, 156106−1.
(20) Gao, H. J.; Ji, W.; Feng, M. J. *Comput. Theory Nanosci.* **2006**, *3*, 970.
(21) Bandyopadhyay, A.; Pal, A. J. *Appl. Phys. Lett.* **2004**, *84*, 999.
(22) Donhauser, Z. J.; Mantooth, B. A.; Kelly, K. F.; Bumm, L. A.; Monnell, J. D.; Stapleton, J. J.; Price, D. W.; Rawlett, A. M.; Allara, D. L.; Tour, J. M.; Weiss, P. S. *Science* **2001**, *292*, 2303.
(23) Grazulevivius, J. V.; Strohrirgl, P.; Pielichowski, J.; Pielichowski, K. *Prog. Polym. Sci.* **2003**, *28*, 1297.
(24) Zhang, Y. D.; Wada, T.; Sasabe, H. *J. Mater. Chem.* **1998**, *8*, 809.
(25) Walsh, C. A.; Burland, D. M. *Chem. Phys. Lett.* **1992**, *195*, 309.
(26) (a) Day, D.; Gu, M.; Smallridge, A. *Adv. Mater.* **2001**, *13*, 1005. (b) Rahn, M. D.; West, D. P.; Khand, K.; Shakos, J. D.; Shelby, R. M. *Appl. Optics* **2001**, *40*, 3395. (c) Darracq, B.; Canva, M.; Chaput, F.; Boilot, J. P.; Riehl, D.; Levy, Y.; Brun, A. *Appl. Phys. Lett.* **1997**, *70*, 292. (d) Wu, S. Z.; Lu, M.; She, W. L.; Yan, K.; Huang, Z. Z. *Mater. Chem. Phys.* **2004**, *83*, 29. (e) Chun, H.; Joo, W. J.; Kim, N. J.; Moon, I. K.; Kim, N. J. *Appl. Polym. Sci.* **2003**, *89*, 368.
(27) Choi, J. S.; Kim, J. H.; Kim, S. H.; Suh, D. H. *Appl. Phys. Lett.* **2006**, *89*, 15211.
(28) Ling, Q. D.; Song, Y.; Ding, S. J.; Zhu, C. X.; Chan, D. S. H.; Kwong, D. L.; Kang, E. T.; Neoh, K. G. *Adv. Mater.* **2005**, *17*, 455.
(29) Teo, E. Y. H.; Ling, Q. D.; Song, Y.; Tan, Y. P.; Wang, W.; Kang, E. T.; Chan, D. S. H.; Zhu, C. X. *Org. Electron.* **2006**, *7*, 173.
(30) Hattori, K.; Wada, Y. J. *Polym. Sci. Pol. Phys.* **1975**, *13*, 1863.
(31) Bossmann, S. H.; Ghatlia, N. D.; Ottaviani, M. H.; Turro, C.; Durr, H.; Turro, N. J. *Synthesis* **1996**, *11*, 1313.

product was extracted by diethyl ether. The corresponding polymer, PVBCz, was then prepared by free-radical polymerization as described above. [FT-IR spectroscopy results (KBr pellet, cm^{-1}): 3052, 3019, 2922, 2855 (ν(C−H) aliphatic); 1484, 1460 (ν(C═C) aromatic); 1212 ν(C−O−C); 1119 (ν(C−H) benzene in styrene); 1018 (ν(C−O−C)); 750, 723 (ν(C−H) carbazole). GPC: $M_w \approx$ 24 000 g mol^{-1}, PDI ≈ 1.7].

Device Fabrication and Characterization. Indium-tin oxide (ITO)-coated glass substrates of 1 × 2 cm in size were precleaned by ultrasonication with water, acetone, and isopropanol, in that order. The polymer memory devices were fabricated by spin-coating polymer films of about 50 nm in thickness on ITO from 10 mg/mL solutions of PVK in toluene and of PMCz and PVBCz in dimethylacetamide, followed by solvent removal in a vacuum chamber at 10^{-5} Torr and 60 °C for 12 h. Thermal evaporation of the aluminum electrodes of about 0.16, 0.04, and 0.0225 mm^2 in area and 0.1 μm in thickness, through a shadow mask, on the polymer film produced the ITO/polymer/Al devices. All electrical characterizations were carried out on devices with an active area of 0.16 mm^2, unless stated otherwise, using a HP 4156A semiconductor parameter analyzer equipped with an Agilent 16440A SMU/pulse generator under ambient conditions. ITO was maintained as the ground electrode. Electrical measurements with a mercury droplet (Hg, 99.9995%, ACS Reagent) as the top electrode, instead of the evaporated Al, were obtained using a Kiethley 238 high-current source measurement unit. Fluorescence spectra of the polymer film in the bistable electrical states of the ITO/polymer/Al device were measured in situ on a Shimadzu RF-5301PC Spectrofluorophotometer, with the external bias across the two electrodes imposed by a HP 6282A DC voltage source. Transmission electron microscopy (TEM) images were obtained on a JEOL JEM 2010F field-emission transmission electron microscope. A thin film of the polymer was first deposited on the surface of the TEM copper grid (Cu grid) by drop-casting from the polymer solution, followed by drying under reduced pressure. A small mercury droplet was then introduced on top to form the Cu grid/polymer/Hg structure. A negative voltage sweep was then applied to the Hg droplet, with the Cu grid as the ground electrode, using the HP 6282A DC voltage source. After removal of the top Hg electrode, the field-induced changes in the polymer thin film were imaged by TEM.

Results and Discussion

While the carbazole groups in poly(*N*-vinylcarbazole) (PVK) are directly attached to the main chain, the carbazole groups in poly(2-(*N*-carbazolyl)ethyl methacrylate) (PMCz) and poly(9-(2-((4-vinylbenzyl)oxy)ethyl)-9*H*-carbazole) (PVBCz) are separated from the main chain by ethylacrylate and benzyloxyethyl spacers, respectively. The chemical structures of the polymers and the schematic diagram of the indium-tin oxide/polymer/aluminum (ITO/polymer/Al) device are shown in Figure 1a and b, respectively. The thickness of the spin-coated polymer layer was about 50 nm, as determined from the edge profile of the atomic force microscopy (AFM) image.

The current density−voltage (J−V) curve of the device fabricated with PVK as the active polymer layer shows the device to be always in a single high-conductivity state, and no conductance switching behavior is observed when the voltage across the device is swept from 0 to −3.0 V, as shown in Figure 2a. In comparison, devices fabricated with PMCz and PVBCz (Figure 2b and c, respectively) exhibit

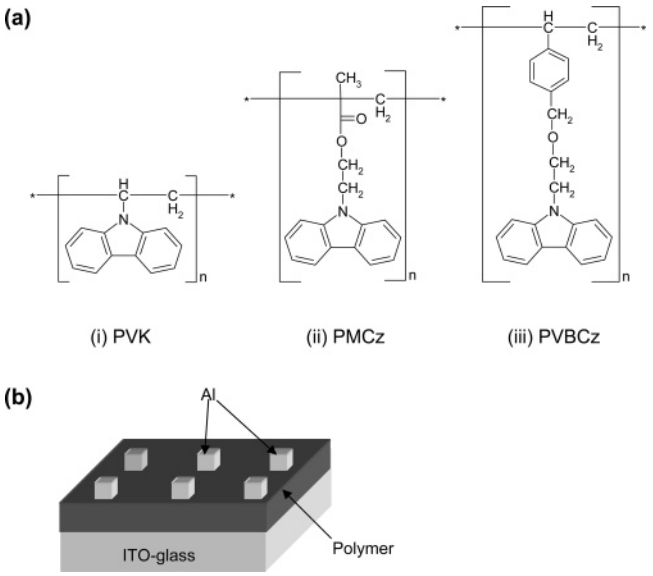

Figure 1. (a) Molecular structures of poly(*N*-vinylcarbazole) (PVK), poly(2-(*N*-carbazolyl)ethyl methacrylate (PMCz), and poly(9-(2-((4-vinylbenzyl)oxy)ethyl)-9*H*-carbazole (PVBCz). (b) Schemetic diagram of the memory device consisting of a thin film (∼50 nm) of the polymer sandwiched between an indium-tin-oxide (ITO) substrate and an aluminum top electrode.

conductance switching associated with the electrical bistability. The electrical and switching characteristics of the ITO/PMCz/Al device have been reported previously.[29] The ITO/PMCz/Al device switches from the low-conductivity (OFF) state to the high-conductivity (ON) state at about −1.8 V when the voltage applied was increased from 0 to −2 V (sweep 1 in Figure 2b) and cannot be returned to its OFF state by subsequent application of a negative bias (sweep 2 in Figure 2b) or a positive bias (not shown). The device remains in the ON-state even after the power has been turned off. The device has an ON/OFF current ratio up to 10^6 when read at −1 V. The ITO/PMCz/Al device thus exhibits write-once-read-many-times (WORM) memory behavior, as it is both non-rewritable and nonvolatile after it has been switched ON. The OFF and ON states are stable both at a constant voltage stress of −1.0 V and up to 10^8 read cycles at −1.0 V.

The ITO/PVBCz/Al device switches from the OFF to ON state at about −2.0 V, with an ON/OFF current ratio of about 10^3, when a voltage sweep from 0 to −3 V was applied (sweep 1 in Figure 2c). The device remains in the ON state when the voltage sweep was repeated (sweep 2). As exemplified by the J−V curve in Figure 2c, the memory device cannot be returned to the OFF state by the application of a reverse bias of the same magnitude after it has been switched ON (sweep 3) and is thus non-rewritable. The memory device was able to remain in the ON state for a period of 2−10 min after turning off the power, after which it can be switched ON again by applying the appropriate voltage (Sweep 4). The memory effect of the device is thus volatile. However, the ON state can be electrically sustained by refreshing pulses of −1 V (pulse width = 10 ms) every 5 s or under a continuous bias of 1 V, as seen in Figure 2c and d, respectively, while maintaining the ON/OFF current ratio at approximately 10^3. Thus, the behavior of the ITO/PVBCz/Al device shares some common characteristics with

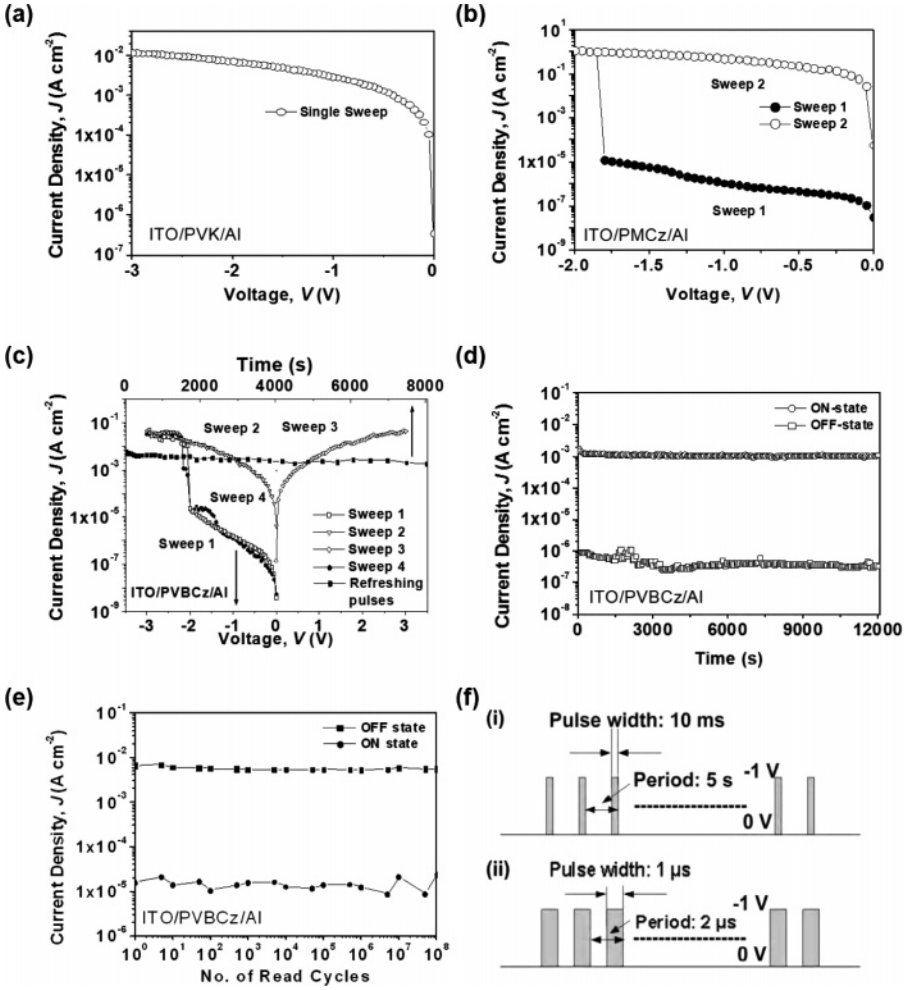

Figure 2. (a) $J-V$ characteristics of an ITO/PVK/Al device showing a single conductivity state. (b and c) $J-V$ characteristics of an ITO/PMCz/Al device and ITO/PVBCz/Al device, respectively, in the OFF and ON state, with the corresponding OFF-to-ON transitions at −1.8 and −2.0 V (part c also shows the ON state being maintained by refreshing at −1 V with a pulse width of 10 ms every 5 s). (d) Stability of the Al/PVBCz/ITO device in either OFF or ON state under a constant stress of −1 V. (e) Effect of read cycles on the OFF and ON states. (e) Pulses used for (i) refreshing the ON state and (ii) read-cycle testing.

that of a static random access memory (SRAM), except for the relatively long retention time (≥2 min) of the ON state. Both the ON and OFF states are also stable up to 10^8 read cycles at a read voltage of −1 V. No resistance degradation is observed for both the ON and OFF states during such testing, as shown in Figure 2e. Figure 2f shows the pulses used (i) for refreshing the ON state and (ii) for the read-cycle testing. Similar switching performances were observed using either an evaporated aluminum-top electrode or a mercury-droplet electrode. This result allows the exclusion of interfacial oxides, metal nanoparticles, or filaments as the origin of the observed conductance switching.[32] Furthermore, the almost linear current−area dependence of both the OFF and ON states when the active device area was reduced from 0.16 to 0.04 to 0.0225 mm^2, giving almost constant current densities, indicate the absence of sample degradation and dielectric breakdown. The conductance switching observed can thus be fully attributed to the change in the material properties of the polymer layer upon applying an external bias. Additional spectroscopic and physical evidence is given below.

The high-conductivity (ON) states of PMCz and PVBCz are likely to be similar to that of poly(*N*-vinylcarbazole) (PVK), since all three polymers have the same carbazole pendant groups and a saturated main chain. The carbazole group is an electron-donor and hole-transporter[23,33,34] and has a tendency to form a partial or full face-to-face conformation with the neighboring carbazole groups to result in extended electron delocalization.[35] Such regions of electron delocalization provide pathways for charge-carrier hopping via the carbazole groups in the direction of the electric field.[23] The switching effect in the PMCz and PVBCz devices probably arises from a change in conformation of the polymers via rotations of the carbazole groups to result in a more regioregular arrangement, similar to that of PVK in Figure 3a. At low applied voltages, the carbazole pendant groups attached to the main chain via flexible C−O linkages in

(32) Caironi, M.; Natali, D.; Sampietro, M.; Bertarelli, C.; Bianco, A.; Dundulachi, A.; Canesi, E.; Zerbi, G. *Appl. Phys. Lett.* **2006**, *89*, 243519−1.

(33) Akcelrud, L. *Prog. Polym. Sci.* **2003**, *28*, 875.

(34) Morin, J. F.; Leclerc, M.; Ades, D.; Siove, A. *Macromol. Rapid Comm.* **2005**, *26*, 761.

(35) Vandendriessche, J.; Palmans, P.; Topet, S.; Boens, N.; De Schryver, F. C.; Masuhara, H. *J. Am. Chem. Soc.* **1984**, *106*, 8057.

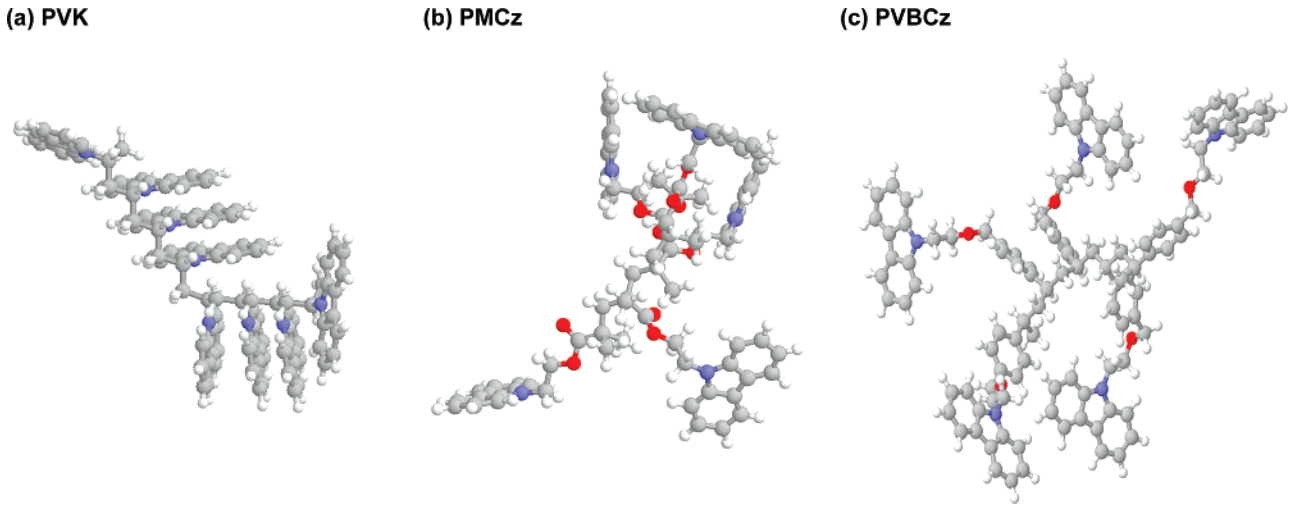

Figure 3. Simulated 3D models by molecular mechanics showing the optimized geometry corresponding to the minimum energy states in (a) PVK, (b) PMCz, and (c) PVBCz.

PMCz and PVBCz are initially in random orientations, as shown by the simulated 3D models from molecular mechanics in Figure 3b and c, respectively. Each optimized geometry corresponds to the minimum energy conformation of the polymer in the low-conductivity or OFF state, and charge-carrier hopping along the carbazole groups is difficult. Under a negative bias, hole injection from ITO oxidizes the carbazole groups near the interface, forming positively charged species. As an effective electron donor, the nearby neutral carbazole groups undergo charge transfer or donor−acceptor interactions with the positively charged carbazole groups to form partial or full face-to-face conformation with the neighboring carbazole groups. The positive charge is then delocalized to the neighboring, ordered carbazole groups. The process can then propagate through the bulk polymer film. When the applied voltage exceeds the threshold value, a significant fraction of the carbazole groups has undergone such a conformational change, resulting in enhanced charge transport through neighboring, aligned carbazole groups either on the same or neighboring polymer chains (intrachain or interchain hopping),[36] producing the high conductivity state (ON state). When the power is turned off, the residual positive charges are localized on the carbazole groups, and the polymer becomes "self-doped". The N 1s X-ray photoelectron core-level spectra obtained from the OFF and ON states of the PMCz device with a detachable mercury electrode show a positive shift in binding energy from 399.7 to 400.1 eV, consistent with the presence of partial positive charges residing on the nitrogen atoms of the carbazole groups. Such carbazole groups with partial positive charges are stabilized by the spacer units containing the electronegative oxygen. Thus, the self-doped state of PMCz is stable, and the regioregular (high conductivity) state can be maintained. The localized partial positive charge on the carbazole nitrogen elevates the highest-occupied-molecular-orbital (HOMO) energy level and lowers the lowest-unoccupied-molecular-orbital (LUMO) energy level of carbazole moieties, resulting in reduced band gap and barrier height with respect to hole injection or electron injection from both electrodes. Therefore, the ON-state $J-V$ curves obtained under both biases are almost symmetrical (Figure 2c), despite the difference in energy barriers for hole injection under different voltage biases (0.6 eV for hole injection into the HOMO from ITO under negative bias and 1.0 eV for hole injection into the HOMO from Al under positive bias).

Devices fabricated from PVK are always in the high-conductivity state, while those from PMCz and PVBCz are at the low-conductivity state initially. Both PMCz and PVBCz devices have comparable turn-ON voltages (−1.8 and −2.0 V, respectively) because both operate on the same mechanistic principles. The switching times of the two devices obtained at room temperature, 1 ms for the PMCz device and 5 ms for PVBCz device, are also comparable. As the pendant groups of the polymer acquire a higher degree of conformational freedom at a higher temperature, they are able to undergo reorientation with less activation energy and greater speed. Thus, the switching time of the device is expected to decrease when the devices are operated at a higher temperature (but lower than the glass transition (T_g) or crystallization temperature (T_c)). Also, the presence of different spacer units in PMCz and PVBCz have negligible effects on their bandgaps, as well as the highest-occupied molecular-orbital (HOMO) and lowest-unoccupied molecular-orbital (LUMO) energy levels, as indicated by UV absorption edge calculations and cyclic voltammetry results, respectively.[37,38] The polymers have a band gap of about 3.5 eV, a HOMO level of about 5.3 eV, and a LUMO level of about 1.8 eV. However, the PVBCz device, in addition to being volatile, has a much lower ON/OFF current ratio than that of the PMCz device. These results are explained below.

The X-ray diffraction (XRD) patterns of the 3 polymers and aluminum are shown in Figure 4 (diffraction peaks at around 9.85, 38.31, 44.18, 64.55, and 77.60 arise from the aluminum sample holder). Two diffraction peaks centered

(36) Safoula, G.; Napo, K.; Bernede, J. C.; Touihri, S.; Alimi, K. *Eur. Polym. J.* **2001**, *37*, 843.
(37) Bredas, J. L.; Silbey, R.; Boudreaux, D. S.; Chance, R. R. *J. Am. Chem. Soc.* **1983**, *105*, 6555.
(38) Lee, Y. Z.; Chen, X. W.; Chen, S. A.; Wei, P. K.; Fann, W. S. *J. Am. Chem. Soc.* **2001**, *123*, 2296.

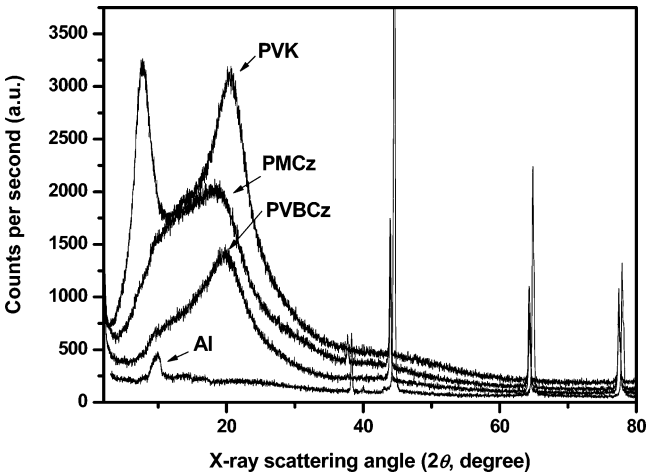

Figure 4. X-ray diffraction patterns of PVK, PMCz, PVBCz, and Al at ground state.

at $2\theta = 20.56°$ (4.316 Å) and 7.76° (11.384 Å) are observed (number in bracket represents the corresponding *d* value for the 2θ peak) for PVK.[39,40] The former peak is an amorphous halo, which is broad, diffuse, and strong, while the latter peak has been shown to be a function of chain parallelism,[41] with the nearest chain-to-chain distance of about 11.38 Å. The result indicates that PVK is regioregular. However, the XRD spectra of PMCz and PVBCz consist of only one broad peak at around $2\theta = 18.73$ (4.734 Å) and 19.77 (4.487 Å), respectively, similar to that at $2\theta = 20.56°$ of PVK. The results suggest that these two polymers are amorphous at the ground state. The XRD results thus indicate that the spacer between the carbazole group and the backbone interferes with the interaction of the carbazole rings in the amorphous polymer, eliminating the unusual degree of chain parallelism and destroying the regioregularity. However, the holes were still the majority carrier in the amorphous polymer,[41] albeit both generation and mobility were substantially reduced, compared to those in the paracrystalline PVK.

The T_g values of PMCz and PVBCz were determined to be 196 and 109 °C, respectively. The values are considerably lower than that of PVK at 210 °C. The high T_g in PVK is the result of conformational stiffness of the carbazole group as its rotation about the C−N bond is highly restricted.[42] Thus, a high degree of crystallinity exists in PVK, and the carbazole groups are predominantly packed in the face-to-face conformations. The device fabricated with PVK as the electroactive layer is therefore always in the high-conductivity state, and no switching behavior is observed with an applied voltage. The introduction of a flexible spacer between the main chain and the carbazole ring renders flexibility and prevents close packing among the polymer chains. The increase in free volume of the polymer has led to a lowering of the T_g.[43] The vinylbenzene group in PVBCz is bulkier than the methacrylate group in PMCz and thus lowers the T_g of the polymer even further.

In the comparison of the chemical structures and memory properties of PMCz and PVBCz, the bulkier spacer between the pendant carbazole group and the backbone in PVBCz allows a larger free volume and a greater degree of conformational freedom, as indicated by a lower T_g, for relaxation through, for example, rotation of the carbazole and phenyl rings about the C−O bond, causing the ON state to be unstable without the continuous application of a bias. Once the externally applied voltage is removed, the carbazole groups in PVBCz return to their original random conformation (OFF state). On the other hand, the neighboring electron-withdrawing O−C═O groups in PMCz further stabilize the positively charged carbazole groups, prolonging the retention of the ON state. Thus, in contrast to the WORM-type behavior exhibited by the PMCz device, the memory effect exhibited by the PVBCz device is volatile.

The proposed mechanism based on conformational effects is supported by in situ fluorescence spectroscopic measurements of the polymer in the devices (through the transparent ITO back contact). The fluorescence emission spectra ($\lambda_{ex} = 342$ nm) of the polymer was measured with and without external bias and normalized to the maximum of the monomeric emission peak of the carbazole chromophore at about 360 nm. The excimeric carbazole species show broad structureless emissions at about 380 and 420 nm.[44−46] The emission at 420 nm is assigned to the sandwich-like excimer fluorescence for the totally eclipsed conformation, and the emission at the shorter wavelength to the second excimer fluorescence caused by partially overlapped structure with only one eclipsed aromatic ring from each carbazole group. For the emission spectrum of the pristine PVBCz device, prior to applying any bias, the peak at about 360 nm is attributed to the monomer fluorescence of the carbazole chromophore (Figure 5a). There is no broad emission at wavelengths longer than the monomer spectrum. Thus, there is no significant excimer formation in PVBCz, even in the neat film. After the device is stressed at −4 V, the polymer film shows broad emission in the longer wavelength region, with increases in emission intensity at 380 and 420 nm, the wavelengths of interest. The appearance of these emission bands is consistent with the formation of two excimeric states under the influence of the electric field. The broadening of the emission peak at about 360 nm also indicates an increase in the types of emitting species in addition to the monomeric chromophores. This phenomenon could be caused by the formation of carbazole excimers in various overlapping states or carbazole−benzene exciplexes. Consistent with the volatile nature of the PVBCz memory device, the fluorescence emission spectrum obtained 10 min after power-off shows only the monomeric emission. A similar electrical stress experiment performed on the PMCz device reveals a slight red-shift of about 5 nm for the monomeric emission peak,

(39) Richards, G. C. *Macromolecules* **1971**, *4*, 379.
(40) Griffiths, C. H.; Okumura, K.; Van Laeken, A. *J. Polym. Sci. Pol. Phys.* **1977**, *15*, 1627.
(41) Griffiths, C. H. *J. Polym. Sci. Pol. Phys.* **1975**, *13*, 1167.
(42) Karali, A.; Dais, P. *Macromolecules* **2001**, *34*, 5547.
(43) Brar, A. S.; Markanday, M. *Polymer* **2005**, *46*, 11527.
(44) Davidson, K.; Soutar, I.; Swanson, L.; Yin, J. *J. Polym. Sci. Pol. Phys.* **1997**, *35*, 963.
(45) Siegoczynski, R. M.; Ejchart, W. *Macromol. Symp.* **2004**, *212*, 575.
(46) Ito, S.; Yamashita, K.; Yamamoto, M.; Nishijima, Y. *Chem. Phys. Lett.* **1985**, *117*, 171.

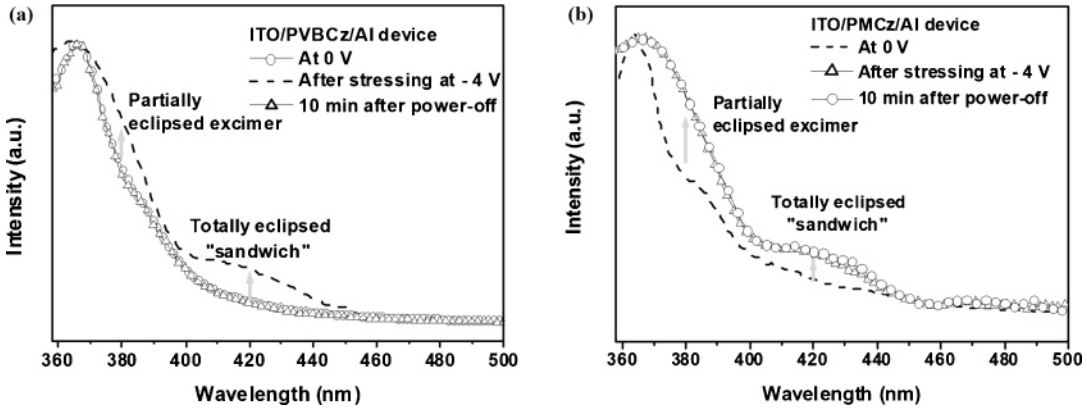

Figure 5. Fluorescence emission spectra showing changes in intensity at ~380 and ~420 nm of the (a) ITO/PVBCz/Al and (b) ITO/PMCz/Al devices at 0 V, after application of a voltage bias and after power-off.

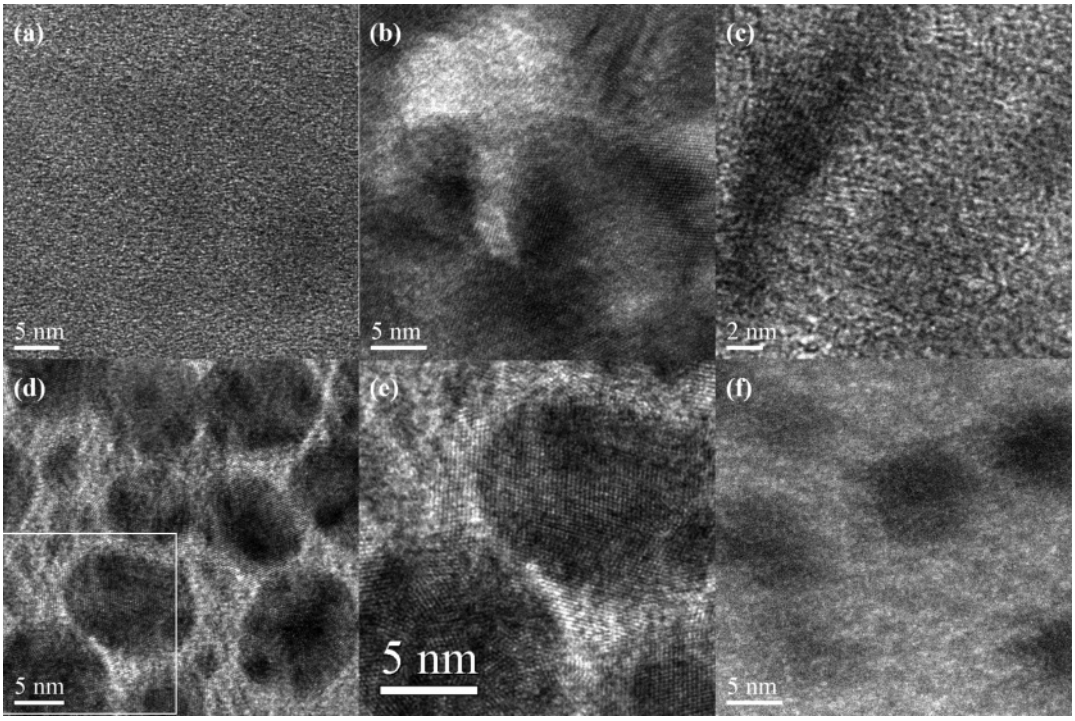

Figure 6. TEM images of (a) a PMCz film without any bias applied (OFF state), (b) a PMCz film showing ordered microdomains after a voltage sweep from 0 to −4 V (ON state), (c) a PMCz film in the ON state with higher magnification, (d) a PVK film, (e) a magnified region in the PVK film, and (f) a PVBCz film, after a voltage sweep from 0 to −4 V and conformation relaxation.

in addition to peak-broadening and increased emissions at about 380 and 420 nm (Figure 5b). The red-shift is indicative of increased electronic delocalization among the carbazole groups in PMCz because the polymer backbone is non-conjugated. In contrast to the PVBCz device, the emission spectrum of the PMCz device remains unchanged (in the excimer state) when measured 10 min after turning off the power, consistent with the nonvolatile nature and WORM behavior of the memory device. It can thus be concluded that the voltage-induced conformation change of the pendant carbazole groups has occurred and is probably responsible for the conductance switching effects observed in the two memory devices.

The "nonvolatile" conformation ordering in the PMCz film in the ON state is also captured in the high-resolution transmission electron microscopy (TEM) images, obtained in a device using a removable Hg droplet as the top electrode and TEM copper grid (Cu grid) as the bottom electrode. A voltage sweep from 0 to −4 V was applied to switch the polymer layer into the ON state. Compared to the TEM image of a PMCz film in the original OFF state (Figure 6a), the image of a PMCz film in the ON state shows ordered microdomains (Figure 6b and c). These ordered domains resemble the polycrystalline structures observed in the images of a poly(*N*-vinylcarbazole) (PVK) film (Figure 6d and e). The TEM images of the PMCz film indicate the appearance of polycrystalline (ordered) structure in the ON state, suggesting that the carbazole pendant groups in PMCz have transformed from a regio-random arrangement, via the field-induced conformation change, to a regio-regular arrangement similar to that of PVK. In comparison, application of a voltage sweep across a PVBCz film does not allow the transformation to regio-regularity to be captured in TEM images because of the volatile nature of the ON state and the difficulty in performing in situ switching during TEM measurements. A representative image of the PVBCz films

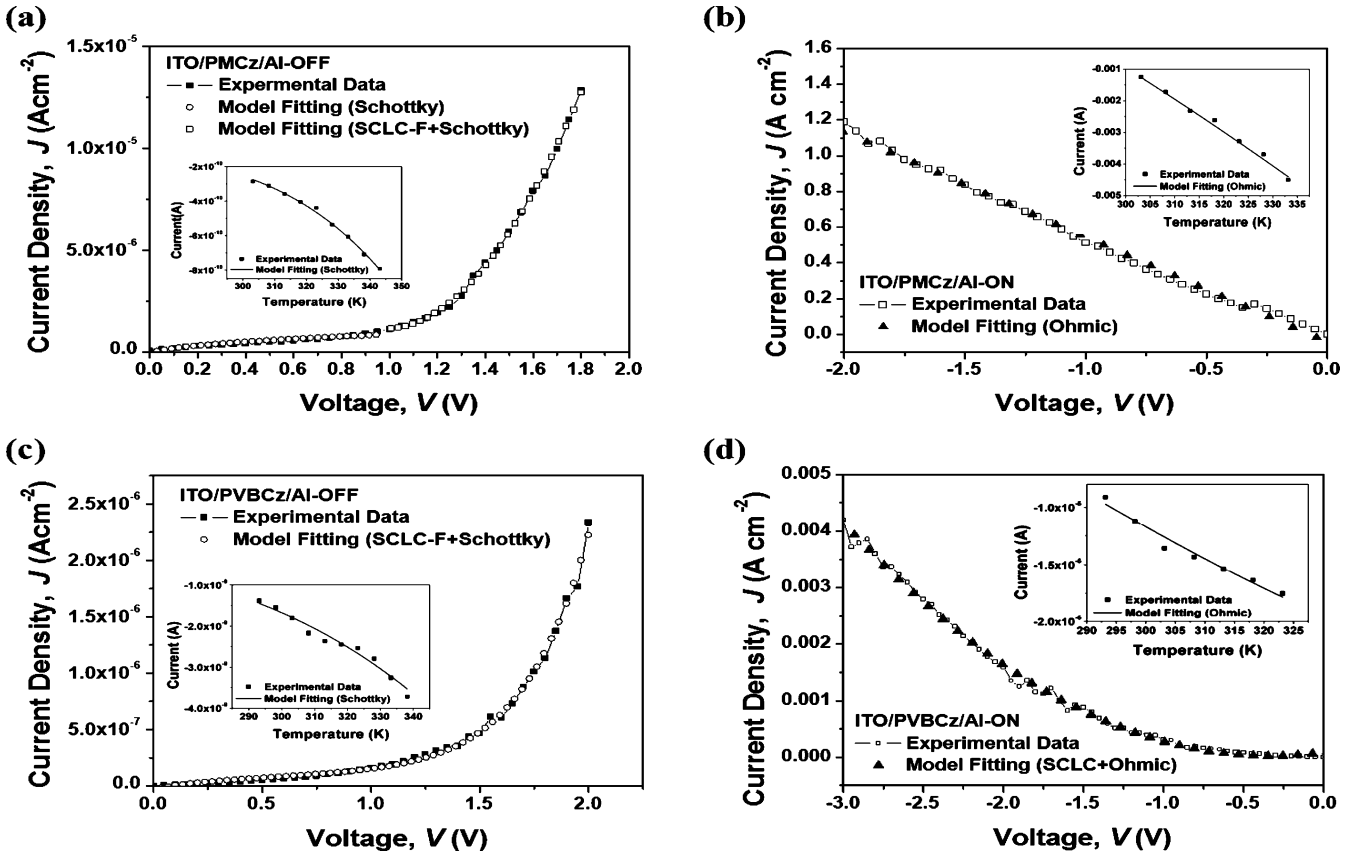

Figure 7. Experimental and fitted $J-V$ curves of ITO/PMCz/Al in the (a) OFF and (b) ON states and of ITO/PVBCz/Al in the (c) OFF and (d) ON states. Inset figures show the temperature dependence of the device currents in accordance to the fitted conduction models. [SCLC-F denotes space-charge-limited current with field dependent mobility]

after the application of an external switching bias in is shown in Figure 6f. The amorphous nature of the film is similar to that of the film in the OFF state. The absence of ordered microdomains is, nevertheless, consistent with the volatile nature of the memory effect of PVBCz, as the conformation relaxation time is much shorter than the sample preparation time (≥ 1 h) for TEM analysis. Therefore, the physical evidence provided by TEM images on field-induced conformation ordering of the pendant carbazole groups in PMCz and PVBCz is in complete agreement with that deduced from the in situ fluorescence spectroscopy results. Because the T_g values (and thus the crystalline melting temperatures) of PMCz and PVBCz are above the temperature induced by Joule heating,[29] the regio-regularity of both polymers are readily retained in the ON state.

The carbazole groups in PMCz overlap to form carbazole−carbazole pairs, similar to the excimeric states in solid PVK films,[47] when they undergo the voltage-induced change in conformation. The carbazole and benzene groups in PVBCz may overlap partially to form the exciplex-like carbazole−benzene−carbazole complexes, in addition to the excimers, as the excited carbazole groups are able to induce the benzene ring into an excited state.[48] An exciplex is formed when a molecule or subunit in an excited-state complexes with a complementary molecule or a subunit in its ground state with no substantial charge separation.[49] The excited species are termed excimers when the two components of the complexes are chemically identical and exciplexes when they are not. Although charge transport among carbazole groups separated by a small number of benzene units can occur,[50] the interspersed benzene groups pose a higher resistance to charge transport, in comparison to transport through pathways formed solely by the carbazole groups. The more amorphous nature of PVBCz also means that the carbazole groups are further apart in the ground state and the charge transport pathways formed by conformational changes may be shorter or less continuous. Thus, the change in conductivity caused by conformational changes in PVBCz is limited. As a result, the ON state current density and the ON/OFF current ratio in PVBCz devices are lower than those in the corresponding PMCz devices. This difference in conformational effect is supported by the fitting of the current density−voltage data to different current transport models. The OFF state $J-V$ curves of both PMCz and PVBCz devices can be fitted well to a combination of the Schottky emission model[51] and the space-charge-limited current model with field-dependent mobility[52] (Figure 7a and c). The latter has been widely used

(47) Slobodyanik, V. V.; Naidyonov, V. P.; Pochinok, V. Y.; Yashchuk, V. N. *Chem. Phys. Lett.* **1981**, *81*, 582.
(48) Ha, H. O.; Lee, G. H.; Suh, H. S.; Lee, J. O.; Cho, W. J.; Ha, C. S. *Synth. Met.* **2001**, *117*, 245.
(49) Jiang, X.; Register, R. A.; Killeen, K. A.; Thompson, M. E.; Pschenitzka, F.; Hebner, T. R.; Sturm, J. C. *J. Appl. Phys.* **2002**, *91*, 6717.
(50) Solaro, R.; Galli, G.; Masi, F.; Ledwith, A.; Chiellini, E. *Eur. Polym. J.* **1983**, *19*, 433.
(51) Sze, S. M. *Physics of Semiconductor Devices*, 2nd ed; Wiley: New York, 1981.
(52) Murgatroyd, P. N. *J. Phys. D* **1970**, *3*, 151−156.

for charge transport in organics. Their respective equations are given by

$$J\alpha T^2 \exp\left[\frac{-q(\phi_B - \sqrt{qV/4\pi\epsilon_i d})}{kT}\right] \quad (1)$$

where ϕ_B is the barrier height, ϵ_i is the insulator permittivity, and d is the insulator thickness, and

$$J\alpha\frac{9}{8}\mu\epsilon_i\frac{V^2}{d^3}\exp\left\{\frac{0.891}{kT}\left(\frac{e^3V}{\pi\epsilon_i d}\right)^{1/2}\right\} \quad (2)$$

where μ is the mobility of the carriers.

The initial current under negative bias, with ITO as the ground electrode and Al as the negative electrode, is injection limited because of the charge-injection barrier present at the ITO interface. Thus the current is dominated by Schottky emission at low voltages. The higher energy barrier for electron injection from the Al contact means that the hole injection from ITO is not balanced by electron injection. As the voltage is increased, the large number of holes readily supplied by the ITO anode results in the flow of current through the device being limited by the buildup of space charges in the polymer layer, and the current is a combination of the Schottky emission and space-charge-limited conduction with field-dependent mobility. At the threshold voltage, there is sufficient energy for the conformation change to occur, and the holes can be easily transported along aligned carbazole groups via hopping, resulting in a surge in current and Ohmic conduction. However, while the $J-V$ curve of PVK[36] and the ON state $J-V$ curve of PMCz device can both be fitted to the Ohmic conduction model[51] (Figure 7b), the ON state $J-V$ curve of the PVBCz device is best fitted to a combination of the space-charge-limited model and the Ohmic model[53] (Figure 7d) as follows

$$J\alpha\frac{9\epsilon_i\mu V^2}{8d^3} + V\exp(-c/T) \quad (3)$$

where μ is the mobility of the carriers and c is a positive constant independent of V or T. This result can be attributed to the presence of benzene units in the charge transport pathways, which are not as efficient at charge transportation and thus limit the current flow.

The appropriateness of the fitted models is confirmed by studying the temperature dependence of the device currents. The currents in the PMCz and PVBCz devices at the OFF and ON states are recorded at different temperatures at a read voltage of -1 V, and the current−temperature data are shown as insets of the corresponding $J-V$ curves in Figure 7a−d. On the basis of the $J-V$ curve of the PMCz device in the OFF state, the Schottky model is dominant at -1 V. The corresponding current−temperature data can be fitted well using the Schottky model, as shown inset of Figure 7a. Similarly, the current−temperature data of the PVBCz device in the OFF state is best fitted based on the Schottky model. This suggests that, although the $J-V$ data of the PVBCz in the OFF state can be fitted well by a combination of the Schottky emission model and the space-charge-limited current model with field dependent mobility, Schottky emission dominates at a low voltage of -1 V. The ON state currents of both the PMCz and PVBCz devices show a dependence on temperature in accordance to the Ohmic model (inset of Figure 7b and d), verifying that the charge conduction in the devices is Ohmic.

Although PVK has the highest degree of regioregularity among the three polymers, the current density of the PVK device, with a single conductivity state, is not significantly higher than the ON state current densities in the PMCz and PVBCz devices. Because the charge transport pathways of aligned carbazole groups in PMCz and PVBCz are formed under the influence of an applied electric field, they are the more direct or optimal routes for the charge transport between the two electrodes. In contrast, the carbazole groups in PVK are unable to respond to the applied electric field to form the optimal charge transport pathways because of the conformational rigidity of the polymer. Nevertheless, the current density of the PVK device is significantly higher than the OFF state current densities of both the PMCz and PVBCz devices by up to 3 orders of magnitude at the corresponding bias voltages.

After they are switched to the ON state, both the PMCz and PVBCz devices could not be returned to the OFF state by application of a reverse bias of magnitude similar to or higher than the switching voltage. This observation is consistent with the mechanism of conformation-induced electrical bistability. Unlike a rewritable memory device operating on a redox or charge-transfer mechanism, in which extra charges can be added or removed by application of an appropriate electric field to return the device to its original state, the present carbazole-containing polymer memories operate on a conformation-induced switching mechanism. Once the conduction pathways are formed under an applied electric field, they facilitate charge transport under both biases, and the device cannot be switched off by application of an opposite bias or a higher voltage of the same bias. The device can only return to the OFF state through conformational relaxation when there is sufficient conformational freedom, as in the case of the PVBCz device. Since the carbazole polymers are hole-transporting polymers, the switching effect and conduction are mainly dependent on the ITO electrode (hole-injecting interface). Consistent with the proposed mechanism, the work function of the top electrode does not have a significant effect on the electrical behavior. The $J-V$ characteristics of the ITO/polymer/Al and ITO/polymer/Hg devices show similar switching behavior, with comparable threshold voltages.

Conclusions

The properties of polymer memory devices, such as the ON/OFF current ratio and retention time, can be tuned even when they are based on materials containing the same functional group responsible for the conductance switching and thus operate via the same switching mechanism. Nonvolatile and volatile conductance switching effects are observed in single-layer memory devices fabricated from non-conjugated polymers with conformationally disordered

(53) Campbell, A. J.; Bradley, D. D. C.; Lidzey, D. G. *J. Appl. Phys.* **1997**, *82*, 6326.

pendant carbazole groups in ethylacrylate and benzyloxyethyl spacer units, respectively. The field-induced conformational ordering and retention of the ordered state in the polymers are elucidated unambiguously from (i) the excimer fluorescence, (ii) the formation of order molecular domains in high-resolution TEM images, (iii) the absence of a switch off mechanism under reverse bias, (iv) the dependence of device volatility on the ease of conformational relaxation of the regioregular pendant carbazole groups, and (v) the dependence of the ON/OFF state current ratio and the ON state conduction mechanism on the degree of regioregularity of the carbazole groups. The extents of regioregularity, conformation ordering, and conformational relaxation, in turn, are dictated by the chemical structure and steric effect of the spacer units between the carbazole moiety and the main chain.

CM071520X